

## Supplementary information

# Effects of $\text{LnF}_3$ on reversible and cyclic hydrogen sorption behaviors in $\text{NaBH}_4$ : Electronegativity of Ln versus crystallographic factors

Lina Chong,<sup>a</sup> Jianxin Zou,<sup>\*ab</sup> Xiaoqin Zeng<sup>ab</sup> and Wenjiang Ding<sup>ab</sup>

<sup>a</sup>National Engineering Research Center of Light Alloys Net Forming & State Key Laboratory of Metal Matrix Composite, Shanghai Jiao Tong University, Shanghai 200240, China.

<sup>b</sup>Shanghai Engineering Research Center of Magnesium Materials, Application & School of Materials Science and Engineering, Shanghai Jiao Tong University, Shanghai 200240, China

### Broader context

Hydrogen is regarded as an ideal energy carrier for future sustainable society. However, the major obstacle to the development of hydrogen economy is the lack of efficient hydrogen storage carrier. Sodium borohydride,  $\text{NaBH}_4$ , as a promising candidate for hydrogen storage, has attracted much attention since the early 2000s due to its high hydrogen content (10.8 wt %), stable to air exposure and low cost. Unfortunately, its application is hindered by the high hydrogen desorption temperature and poor reversibility. This work demonstrates the dramatic improvements in de-/rehydrogenation thermodynamics and kinetics of  $\text{NaBH}_4$  through the addition of lanthanide trifluorides as reagent. All the studied  $3\text{NaBH}_4\text{-LnF}_3$  ( $\text{Ln} = \text{La, Ce, Pr, Nd, Sm, Gd, Ho, Er}$  and  $\text{Yb}$ ) composites show reversible hydrogen storage ability but different sorption behaviors. The best overall performances, including suitable thermodynamics, rapid kinetics and high capacity, are achieved in the  $3\text{NaBH}_4\text{-GdF}_3$  composite. In particular, the composite shows high cycling stability over 51 cycles with fast kinetics and can be still rehydrogenated under moderate conditions (182 °C, 1 MPa). The hydrogen sorption behaviors of  $3\text{NaBH}_4\text{-LnF}_3$  composites are correlated with the electronegativities of the  $\text{Ln}^{3+}$  cations, their electron configurations and the geometric factors of Ln-B phases. This work provides us with some criterions for optimizing the hydrogen storage performances of metal borohydrides based hydrogen storage systems.

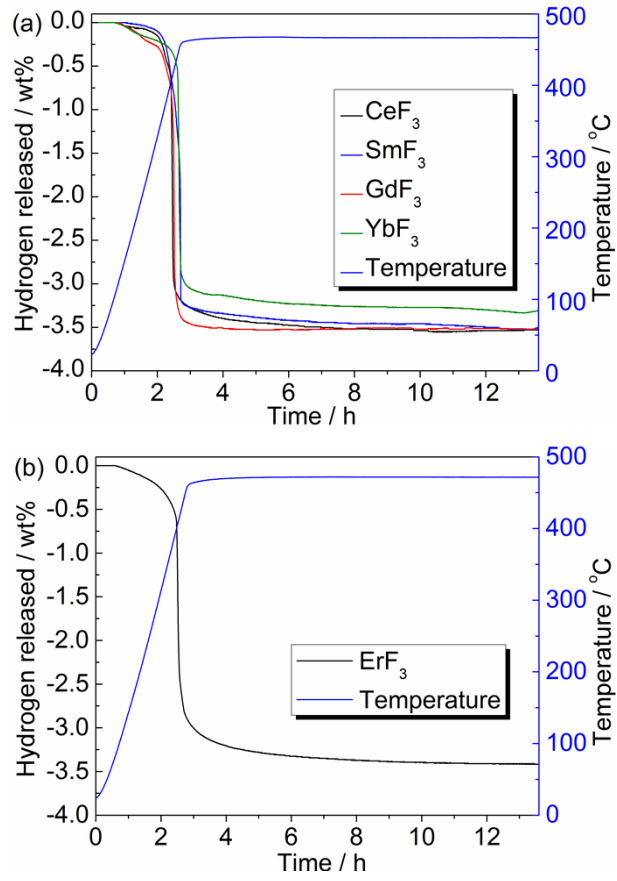


Fig. S1. Temperature-programmed-desorption (TPD) profiles of (a) the  $3\text{NaBH}_4\text{-CeF}_3$ ,  $3\text{NaBH}_4\text{-SmF}_3$ ,  $3\text{NaBH}_4\text{-GdF}_3$  and  $3\text{NaBH}_4\text{-YbF}_3$  composites, (b) the  $3\text{NaBH}_4\text{-ErF}_3$  composite. Heating rate is  $3\text{ }^\circ\text{C min}^{-1}$ .

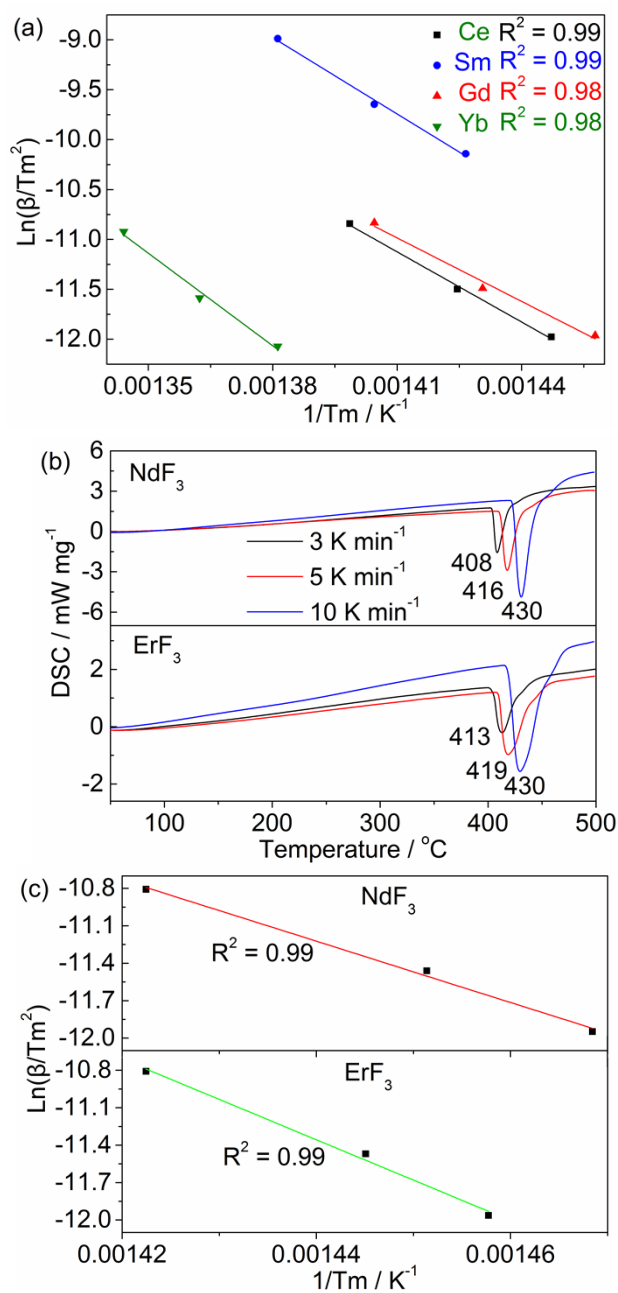


Fig. S2. (a) Kissinger plots of the dehydrogenation of the  $3NaBH_4-CeF_3$ ,  $3NaBH_4-SmF_3$ ,  $3NaBH_4-GdF_3$  and  $3NaBH_4-YbF_3$  composites. Data obtained from DSC measurements (Fig. 1). (b) DSC curves of  $3NaBH_4-NdF_3$  and  $3NaBH_4-ErF_3$  composites with heating rate being 3, 5, 10 K  $min^{-1}$  under 1 bar argon atmosphere, respectively; (c) Kissinger plots corresponding to (b).

Table S1. The peak temperatures corresponding to the four composites at different heating rates under 1 bar argon atmosphere.

| Sample                               | Heating rate / K<br>min <sup>-1</sup> | Peak temperature / °C | H <sub>2</sub> released / wt% |
|--------------------------------------|---------------------------------------|-----------------------|-------------------------------|
| 3NaBH <sub>4</sub> -CeF <sub>3</sub> | 3                                     | 418                   | 3.33                          |
|                                      | 5                                     | 429                   |                               |
|                                      | 10                                    | 442                   |                               |
| 3NaBH <sub>4</sub> -SmF <sub>3</sub> | 3                                     | 426                   | 3.43                          |
|                                      | 5                                     | 439                   |                               |
|                                      | 10                                    | 453                   |                               |
| 3NaBH <sub>4</sub> -GdF <sub>3</sub> | 3                                     | 416                   | 3.45                          |
|                                      | 5                                     | 426                   |                               |
|                                      | 10                                    | 436                   |                               |
| 3NaBH <sub>4</sub> -YbF <sub>3</sub> | 3                                     | 449                   | 3.01                          |
|                                      | 5                                     | 463                   |                               |
|                                      | 10                                    | 476                   |                               |

Table S2. The onset dehydrogenation temperatures - $T_{on}$ , temperatures for the maximum desorption rates -  $T_p$  and dehydrogenation activation energies ( $E_a$ ) of 3NaBH<sub>4</sub>-LnF<sub>3</sub> (Ln = La, Ce, Pr, Nd, Sm, Gd, Ho, Er, Yb) composites obtained from TPD<sup>a</sup> and DSC<sup>b</sup> measurements, respectively.

| Sample                               | $T_{on}$ / °C <sup>a</sup> | $T_p$ / °C <sup>b</sup> | $E_a$ / kJ mol <sup>-1</sup> <sup>b</sup> |
|--------------------------------------|----------------------------|-------------------------|---|
| 3NaBH <sub>4</sub> -LaF <sub>3</sub> | 160                        | 432                     | 220.1 <sup>1</sup>                        |
| 3NaBH <sub>4</sub> -CeF <sub>3</sub> | 150                        | 418                     | 194.8                                     |
| 3NaBH <sub>4</sub> -PrF <sub>3</sub> | 110                        | 419                     | 235.3 <sup>2</sup>                        |
| 3NaBH <sub>4</sub> -NdF <sub>3</sub> | 80                         | 408                     | 101.8                                     |
| 3NaBH <sub>4</sub> -SmF <sub>3</sub> | 212                        | 426                     | 211.9                                     |
| 3NaBH <sub>4</sub> -GdF <sub>3</sub> | 112                        | 416                     | 176.2                                     |
| 3NaBH <sub>4</sub> -HoF <sub>3</sub> | 86                         | 426                     | 153.0 <sup>3</sup>                        |
| 3NaBH <sub>4</sub> -ErF <sub>3</sub> | 82                         | 413                     | 103.3                                     |
| 3NaBH <sub>4</sub> -YbF <sub>3</sub> | 156                        | 449                     | 257.2                                     |

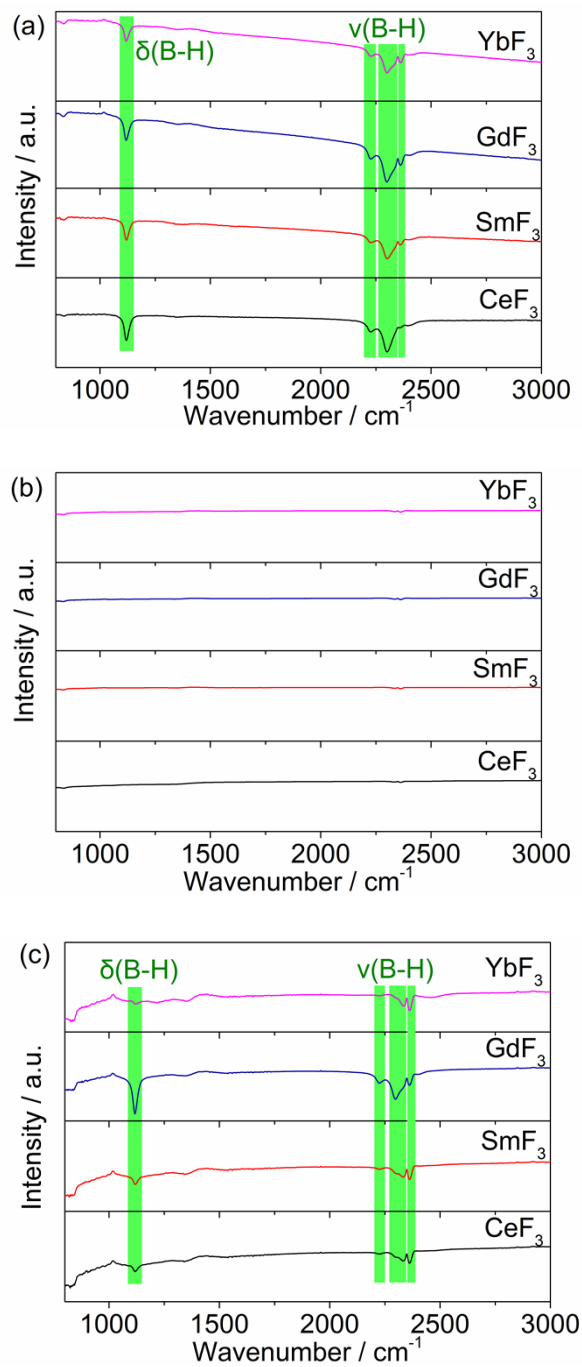


Fig. S3 FTIR patterns of the  $3\text{NaBH}_4\text{-CeF}_3$ ,  $3\text{NaBH}_4\text{-SmF}_3$ ,  $3\text{NaBH}_4\text{-GdF}_3$  and  $3\text{NaBH}_4\text{-YbF}_3$  composites in their corresponding as-prepared (a), dehydrogenated (b) and rehydrogenated (c) states.

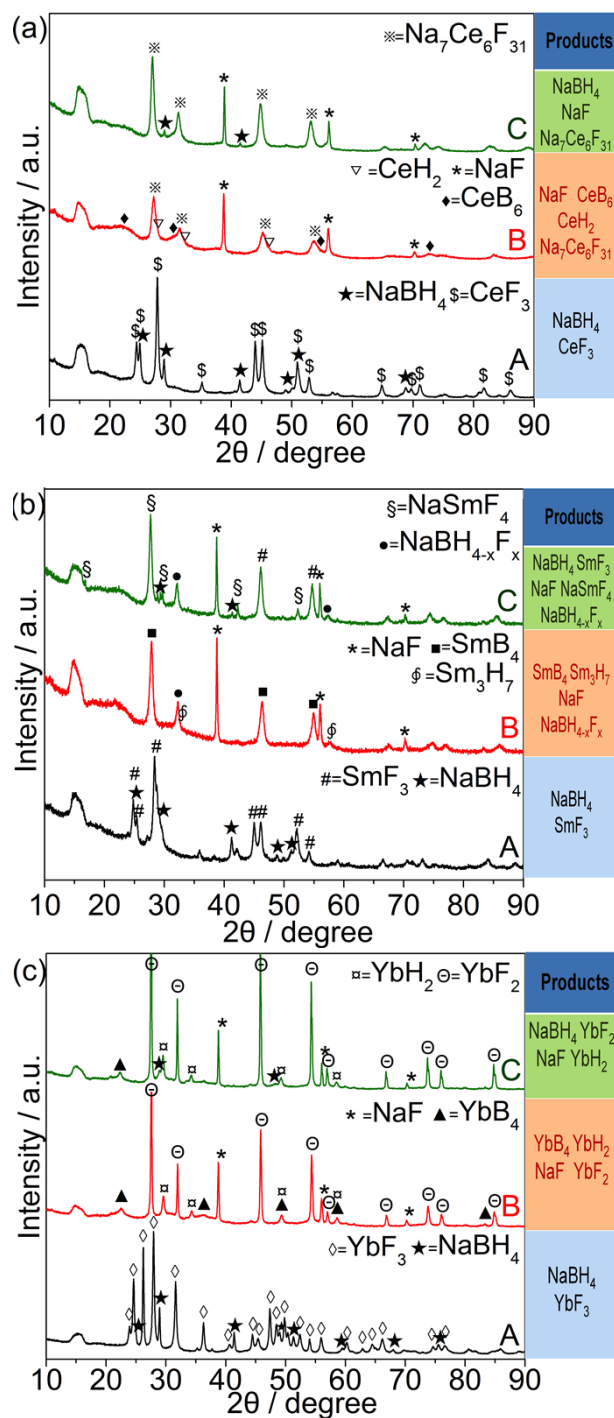
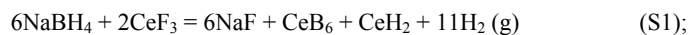


Fig. S4. XRD patterns of  $3\text{NaBH}_4\text{-CeF}_3$  (a),  $3\text{NaBH}_4\text{-SmF}_3$  (b) and  $3\text{NaBH}_4\text{-YbF}_3$  (c) in: as-prepared (line A); dehydrogenated (line B); rehydrogenated (line C) states.

Fig. S4a proved that no new phases formed in the three composites after ball milling, and the characteristic peaks assigned to  $\text{NaBH}_4$  were further demonstrated in FTIR spectra (Fig. S3a). After dehydrogenation, besides the newly formed  $\text{NaF}$  in the three composites, the phases present in the dehydrided  $3\text{NaBH}_4\text{-CeF}_3$ ,  $3\text{NaBH}_4\text{-SmF}_3$  and  $3\text{NaBH}_4\text{-YbF}_3$  composites are  $\text{CeB}_6$ ,  $\text{CeH}_2$  and  $\text{Na}_7\text{Ce}_6\text{F}_{31}$ ;  $\text{SmB}_4$  and  $\text{Sm}_3\text{H}_7$ ;  $\text{YbH}_2$  and  $\text{YbF}_2$ ; respectively. Analyses by FTIR further corroborated the complete decomposition of  $\text{NaBH}_4$  in the three dehydrogenated composites (Fig. S3b). Therefore, based on XRD, FTIR combined with calculation by using

HSC Chemistry program (Fig. S5), the dehydrogenation reactions of the three composites can be deduced as follows:



According to reactions S1-S3, the theoretical hydrogen release contents of 3NaBH<sub>4</sub>-CeF<sub>3</sub>, 3NaBH<sub>4</sub>-SmF<sub>3</sub> and 3NaBH<sub>4</sub>-YbF<sub>3</sub> composites are 3.54, 3.58 and 3.31 wt%, respectively, in a good agreement with the results determined by DSC and TPD measurements. Hence, the formations of Na<sub>7</sub>Ce<sub>6</sub>F<sub>31</sub> and YbF<sub>2</sub> are probably attribute to the side reactions between LnF<sub>3</sub> (Ln = Ce, and Yb) and a small amount of impurity introduced during sample preparation, since Ce<sup>3+</sup> and Yb<sup>3+</sup> have the tendency to be in +4 and +2 states, respectively, which are determined by their special electron configurations.<sup>4</sup>

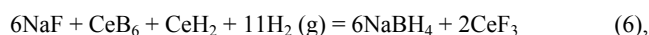
After hydrogen absorption (Fig. S4(c)), the reappearance of peaks corresponding NaBH<sub>4</sub> was observed in the rehydrogenated 3NaBH<sub>4</sub>-CeF<sub>3</sub>, 3NaBH<sub>4</sub>-SmF<sub>3</sub> and 3NaBH<sub>4</sub>-YbF<sub>3</sub> composites, which proved the reversibilities of those composites. FTIR results further clarified the regeneration of NaBH<sub>4</sub> (Fig. S3(c)). Fig. S4c also confirmed the weakened diffraction peaks of NaF in the rehydrogenated 3NaBH<sub>4</sub>-CeF<sub>3</sub>, 3NaBH<sub>4</sub>-SmF<sub>3</sub> and 3NaBH<sub>4</sub>-YbF<sub>3</sub> composites. In addition, besides that the diffraction peaks corresponding to YbH<sub>2</sub> become weak in the rehydrogenated 3NaBH<sub>4</sub>-YbF<sub>3</sub>, no Ln-B or Ln-H phases can be identified in other two rehydrogenated composites. In the case of 3NaBH<sub>4</sub>-SmF<sub>3</sub> composite, apart from the newly formed SmF<sub>3</sub>, NaSmF<sub>4</sub> was also detected. Therefore, the rehydrogenation pathway in the 3NaBH<sub>4</sub>-SmF<sub>3</sub> composite can be proposed as follows:



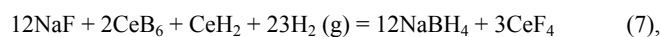
together with a side reaction:



However, no CeF<sub>3</sub> or YbF<sub>3</sub> phases are detected in the rehydrogenated 3NaBH<sub>4</sub>-CeF<sub>3</sub> and 3NaBH<sub>4</sub>-YbF<sub>3</sub> composites. Since HSC Chemistry program can provide reliable thermodynamic parameters of a chemical reaction as a function of temperature,<sup>5</sup> it is therefore used to calculate the Gibbs free energy of the rehydrogenation reaction in the 3NaBH<sub>4</sub>-CeF<sub>3</sub> composite. NaF, CeB<sub>6</sub> and CeH<sub>2</sub> can react with H<sub>2</sub> to form NaBH<sub>4</sub> according to the following formulas:

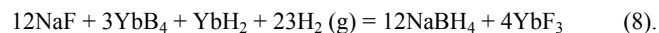


With  $\Delta G = -241.575 \text{ kJ mol}^{-1}$  at 25 °C;



With  $\Delta G = 550.778 \text{ kJ mol}^{-1}$  at 25 °C.

From the thermodynamic point of view, reaction (6) is more favorable at 25°C. The absence of CeF<sub>3</sub> or CeF<sub>4</sub> in the rehydrogenated products is probably due to the side reaction between Ce fluoride and NaF. Similarly, for the 3NaBH<sub>4</sub>-YbF<sub>3</sub> composite, the hydrogen absorption reaction may be proposed as:



Equilibrium compositions for  $3\text{NaBH}_4\text{-CeF}_3$  decomposition.

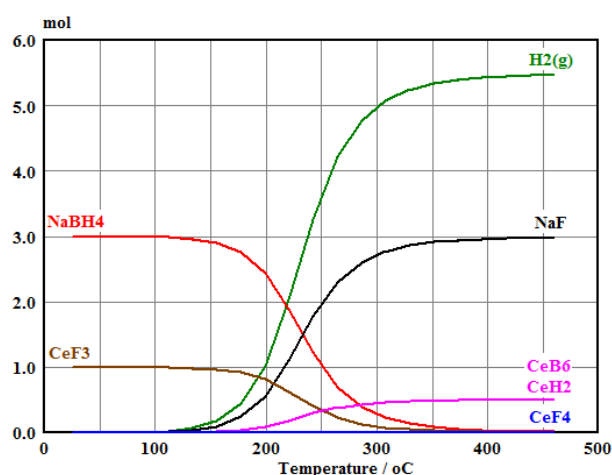


Fig. S5 Equilibrium compositions diagram for the decomposition of  $3\text{NaBH}_4\text{-CeF}_3$  composite, as a function of temperature. The calculation was done using HSC5 software.<sup>5</sup>

The graph shows that no  $\text{CeF}_4$  is formed during dehydrogenation reaction between  $\text{NaBH}_4$  and  $\text{CeF}_3$ . Note that approximately 5.496 mole  $\text{H}_2$  (~3.54 wt% for the composite, ~10.8 wt% for  $\text{NaBH}_4$ ) is released, meanwhile, the mole ratio of  $\text{NaBH}_4\text{:CeF}_3\text{:H}_2\text{:NaF:CeB}_6\text{:CeH}_2$  is 3:1:5.496:2.987:0.498:0.498, in line with our experimental result, which evidences the validity of reaction S1. Because of the formation of  $\text{Na}_7\text{Ce}_6\text{F}_{31}$  resulting from the combination between  $\text{NaF}$  and  $\text{CeF}_4$ , there should be a side reaction between  $\text{CeF}_3$  and a small amount of impurity introduced during sample preparation to yield  $\text{CeF}_4$ , consequently leads to the formation of  $\text{Na}_7\text{Ce}_6\text{F}_{31}$ . On the other hand, this result reveals that  $\text{Na}_7\text{Ce}_6\text{F}_{31}$  is only the by-product.

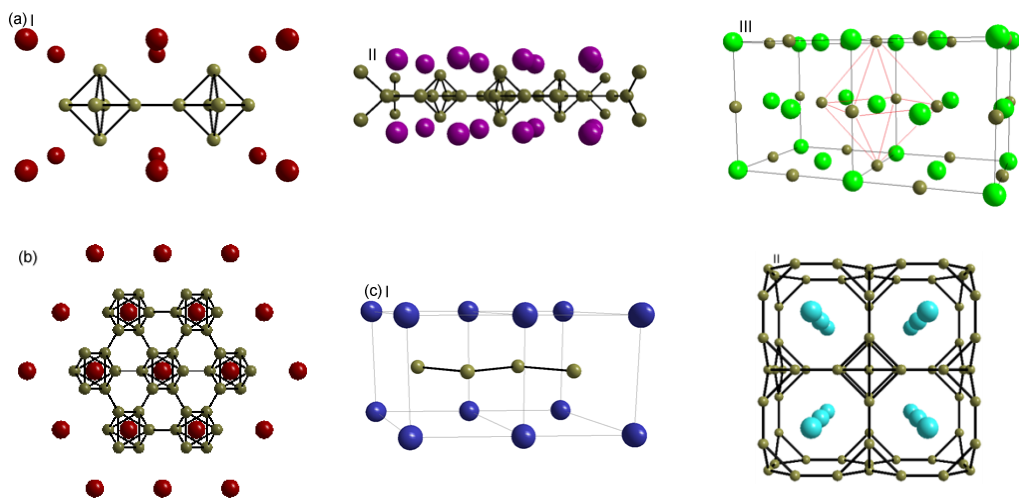


Fig. S6 Schematic representations of (a): (I)  $\text{LnB}_6$  ( $\text{Ln} = \text{La}, \text{Ce}, \text{Pr}$  and  $\text{Nd}$ ) (100) surface, (II)  $\text{LnB}_4$  ( $\text{Ln} = \text{Sm}, \text{Gd}, \text{Ho}$  and  $\text{Yb}$ ) (010) surface, (III) crystal structure of cubic  $\text{NaBH}_4$  ( $\text{Fm-3m}$ ); (b):  $\text{LnB}_6$  (111) surface; (c): crystal structure of (I)  $\text{TiB}_2$ ,  $\text{MgB}_2$  and  $\text{AlB}_2$ ; (II)  $\text{CaB}_6$ . Red ball = La, Ce, Pr and Nd; purple ball = Sm, Gd, Ho and Yb; brown ball = B; green ball = Na; dark blue ball = Ti, Mg and Al; azure ball = Ca.

Table S3. The conditions needed for the transformation from some metal-borides to metal borohydrides.

| Metal boride                                  | Recombined borohydrides | Temperature / °C | Pressure / MPa | Time / h | Reference                |
|---|-------------------------|------------------|----------------|----------|--------------------------|
| TiB <sub>2</sub>                              | LiBH <sub>4</sub>       | 350              | 10             | 12       | 6                        |
| MgB <sub>2</sub>                              | NaBH <sub>4</sub>       | 400              | 35             | 24       | 7                        |
| MgB <sub>2</sub>                              | LiBH <sub>4</sub>       | 390              | 6              | 20       | 8                        |
| AlB <sub>2</sub>                              | LiBH <sub>4</sub>       | 350              | 15             | 50       | 9                        |
| CaB <sub>6</sub> (TiCl <sub>3</sub> catalyst) | LiBH <sub>4</sub>       | 400              | 10             | 20       | 10                       |
| Ln-B  | NaBH <sub>4</sub>       | ~ 400            | ~ 3            | ~ 6      | 1, 2, 3,11 and this work |

Table S4 Comparisons of the electronegativity of Ln<sup>3+</sup>, as well as the dehydrogenation enthalpies ( $\Delta H_d$ ) / rehydrogenation enthalpies ( $\Delta H_f$ ) of 3NaBH<sub>4</sub>-LnF<sub>3</sub> composites for the 1<sup>st</sup> de-/rehydrogenation. Corresponding data were obtained from Ref. 12, DSC<sup>a</sup> and PCT<sup>b</sup> measurements, unless otherwise noted.

| Sample                               | $\chi_p$ of Ln cation <sup>12</sup> | $\Delta H_d$ / kJ mol <sup>-1</sup> <sup>1</sup> H <sub>2</sub> <sup>a</sup> | $\Delta H_f$ / kJ mol <sup>-1</sup> H <sub>2</sub> <sup>b</sup> |
|--------------------------------------|-------------------------------------|--|---|
| 3NaBH <sub>4</sub> -LaF <sub>3</sub> | 1.327(+3)                           | 50.1   | -31.8 <sup>1</sup>  |
| 3NaBH <sub>4</sub> -CeF <sub>3</sub> | 1.348(+3)<br>1.608(+4)              | 46.3   |   |
| 3NaBH <sub>4</sub> -PrF <sub>3</sub> | 1.374(+3)<br>1.646(+4)              | 49.6   | -18.4 <sup>2</sup>  |
| 3NaBH <sub>4</sub> -NdF <sub>3</sub> | 1.382(+3)                           | 50.5   | -13.2 <sup>11</sup>   |
| 3NaBH <sub>4</sub> -SmF <sub>3</sub> | 1.410(+3)                           | 47.6   |   |
| 3NaBH <sub>4</sub> -GdF <sub>3</sub> | 1.386(+3)                           | 53.1   | -15.6   |
| 3NaBH <sub>4</sub> -HoF <sub>3</sub> | 1.433(+3)                           | 47.3   | -27.12 <sup>3</sup>   |
| 3NaBH <sub>4</sub> -ErF <sub>3</sub> | 1.438(+3)                           | 51.4   | -31.7   |
| 3NaBH <sub>4</sub> -YbF <sub>3</sub> | 1.479(+3)<br>1.237(+2)              | 53.8   |   |

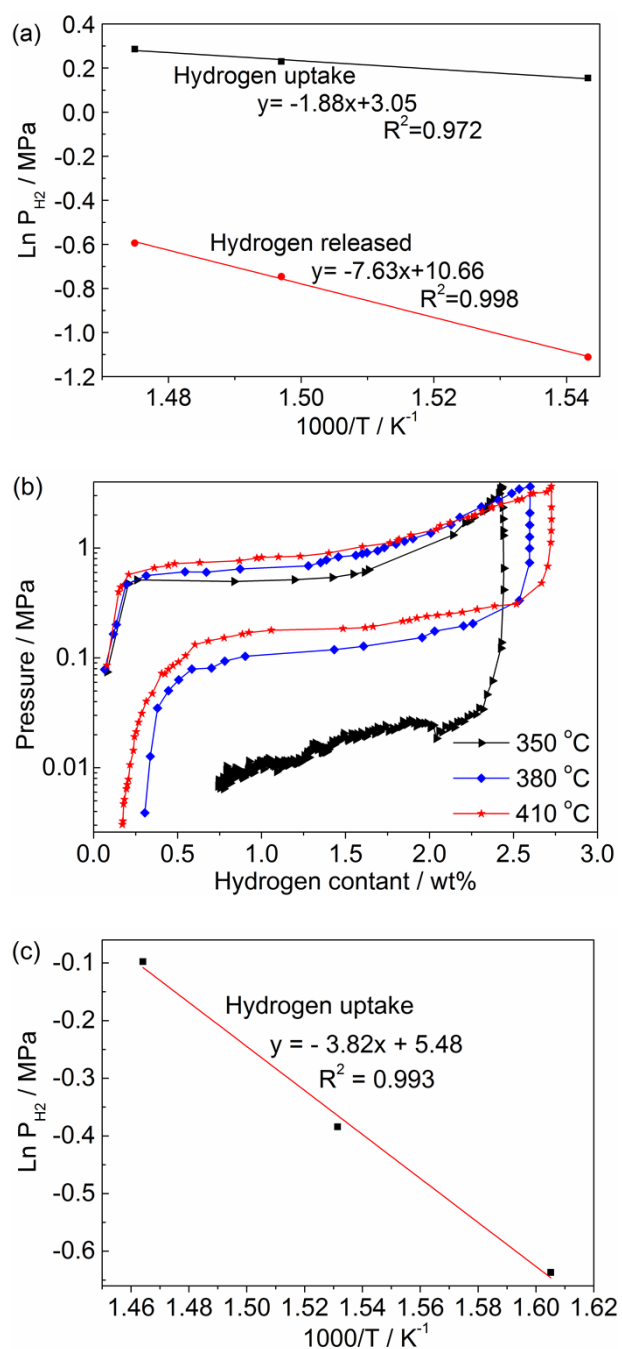


Fig. S7 (a) van't Hoff plots for  $3\text{NaBH}_4\text{-GdF}_3$  composite. Data obtained from PCT measurements of  $3\text{NaBH}_4\text{-GdF}_3$  composite (Fig. 3-down). (b) PCT curves of the  $3\text{NaBH}_4\text{-ErF}_3$  composite measured at 350, 380 and 410 °C. (c) van't Hoff diagrams corresponding to (b).

The hysteresis between absorption and desorption isotherms are also observed in the  $3\text{NaBH}_4\text{-LnF}_3$  ( $\text{Ln} = \text{Ce}, \text{Sm}, \text{Gd}, \text{Er}, \text{Yb}$ ) composites, which may arise from different reaction ways during de-/rehydrogenation, as reported in the study of  $3\text{NaBH}_4\text{-NdF}_3$  system.<sup>11</sup>

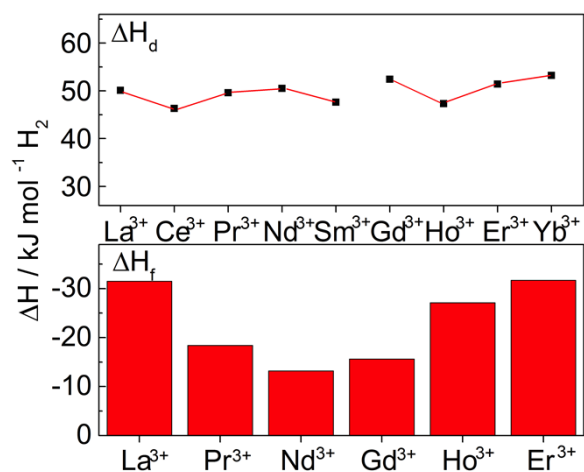


Fig. S8 Relationships between the dehydrogenation(up)/rehydrogenation (down) enthalpies ( $\Delta H_d/\Delta H_r$ ) and the  $\text{Ln}^{3+}$  cations, respectively.

Table S5. Hydrogen storage properties of  $3\text{NaBH}_4\text{-LnF}_3$  composites obtained from PCT measurements.

| Composite                     | Operable cyclic temperature by PCT / °C | Rehydrogenation equilibrium pressure / MPa | Degree of reversibility / % |
|-------------------------------|---|--|-----------------------------|
| $3\text{NaBH}_4\text{-LaF}_3$ | 385                                     | 2.10                                       | 92.7 <sup>1</sup>           |
| $3\text{NaBH}_4\text{-CeF}_3$ | 410                                     | unachievable                               | 42.0                        |
| $3\text{NaBH}_4\text{-PrF}_3$ | 380                                     | 1.923                                      | 82.2 <sup>2</sup>           |
| $3\text{NaBH}_4\text{-NdF}_3$ | 360                                     | 1.463                                      | 84.3 <sup>11</sup>          |
| $3\text{NaBH}_4\text{-SmF}_3$ | 410                                     | unachievable                               | 52.8                        |
| $3\text{NaBH}_4\text{-GdF}_3$ | 350                                     | 1.17                                       | 96.3                        |
| $3\text{NaBH}_4\text{-HoF}_3$ | 400                                     | 2.62                                       | 65.7 <sup>3</sup>           |
| $3\text{NaBH}_4\text{-ErF}_3$ | 410                                     | 0.902                                      | 79.4                        |
| $3\text{NaBH}_4\text{-YbF}_3$ | 410                                     | unachievable                               | 43.4                        |

Table S6. Data obtained from the cycling tests on the 3NaBH<sub>4</sub>-GdF<sub>3</sub> composite.

| Cycle No. | Hydrogenation conditions / °C /MPa | Approx. hydrogenation time / h | wt% H <sub>2</sub> | Cycle No. | Hydrogenation conditions / °C /MPa | Approx. hydrogenation time / h | wt% H <sub>2</sub> |
|-----------|------------------------------------|--------------------------------|--------------------|-----------|------------------------------------|--------------------------------|--------------------|
| 1-6       | 400/3                              | 2                              | 3.50               | 29        | 400/4                              | 3.6                            | 3.48               |
| 7         | 400/3                              | 2.1                            | 3.48               | 30        | 400/3                              | 3                              | 2.45               |
| 8         | 350/3                              | 4.4                            | 2.86               | 31        | 400/2                              | 5.8                            | 1.78               |
| 9         | 400/3                              | 8.8                            | 3.46               | 32        | 400/3                              | 2                              | 2.45               |
| 10        | 400/3                              | 8.3                            | 3.49               | 33        | 400/3                              | 2                              | 2.25               |
| 11        | 310/3                              | 9.2                            | 2.32               | 34        | 400/3                              | 4.7                            | 2.62               |
| 12        | 230/3                              | 7.7                            | 1.82               | 35        | 400/3                              | 2                              | 2.10               |
| 13        | 400/3                              | 2                              | 2.76               | 36        | 400/1                              | 10                             | 1.16               |
| 14        | 400/3                              | 2                              | 2.70               | 37        | 400/4                              | 3                              | 3.48               |
| 15        | 400/3                              | 3.4                            | 3.47               | 38        | 400/3                              | 5.1                            | 2.79               |
| 16        | 400/3                              | 2                              | 2.63               | 39        | 400/3                              | 2                              | 2.13               |
| 17        | 186/3                              | 6.2                            | 1.63               | 40        | 400/3                              | 4.7                            | 2.69               |
| 18        | 400/3                              | 2                              | 1.97               | 41        | 400/3                              | 2                              | 2.28               |
| 19        | 400/3                              | 2                              | 1.97               | 42        | 244/2                              | 5.6                            | 1.40               |
| 20        | 400/3                              | 7.3                            | 3.22               | 43        | 400/4                              | 5.3                            | 3.13               |
| 21        | 400/3                              | 2                              | 2.05               | 44        | 182/1                              | 7.1                            | 0.68               |
| 22        | 400/3                              | 2.1                            | 2.09               | 45        | 400/4                              | 8                              | 2.99               |
| 23        | 400/3                              | 2                              | 2.04               | 46        | 400/4                              | 3                              | 2.69               |
| 24        | 400/3                              | 2                              | 2.01               | 47        | 400/3                              | 3.9                            | 2.29               |
| 25        | 400/3                              | 2                              | 2.11               | 48        | 400/3                              | 5.1                            | 2.52               |
| 26        | 400/1                              | 3                              | 0.82               | 49        | 400/3                              | 5.1                            | 2.50               |
| 27        | 400/2                              | 5.8                            | 1.74               | 50        | 400/3                              | 2                              | 1.96               |
| 28        | 400/3                              | 3                              | 2.47               | 51        | 400/2                              | 3.5                            | 1.46               |

Before the isothermal dehydrogenation measurement, the rehydrogenated sample was firstly cooled to ambient temperature and then pressurized with 5 MPa hydrogen. After the temperature was quickly raised to and kept at the desired one, the sample chamber was quickly evacuated.

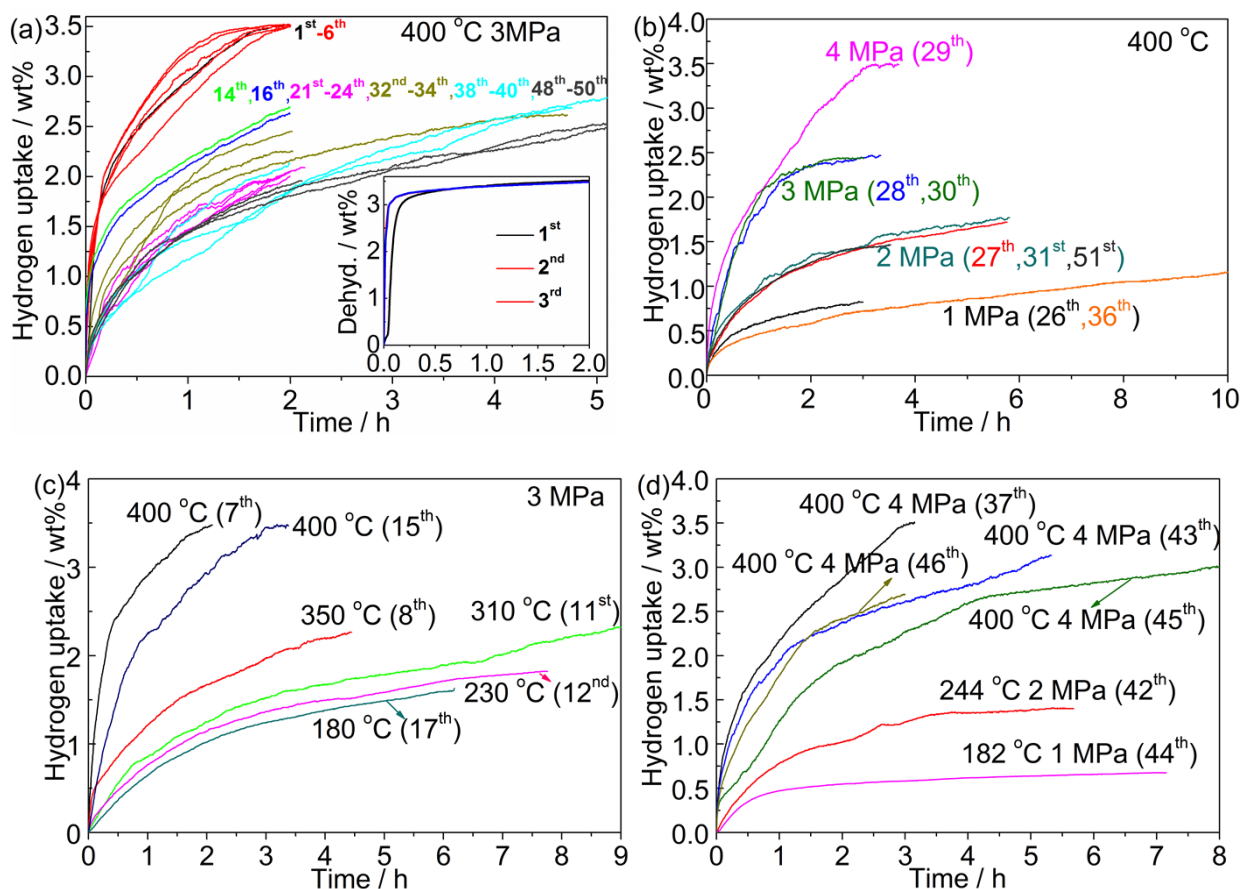


Fig. S9 Rehydrogenation curves of the  $3\text{NaBH}_4\text{-GdF}_3$  composite during cyclic tests under different conditions: (a) 3 MPa-400 °C, inset figure shows the dehydrogenation cyclic curves at 400 °C for the 1<sup>st</sup>, 2<sup>nd</sup> and 3<sup>rd</sup> cycles; (b) 1, 2, 3 and 4 MPa hydrogen pressures at 400 °C; (c) 3 MPa hydrogen pressure at different temperatures; (d) 4 MPa-400 °C, 2 MPa-244 °C and 1 MPa-182 °C.

Inset of Fig. S9(a) displays a fast dehydrogenation kinetics of  $3\text{NaBH}_4\text{-GdF}_3$  composite. For example, the time needed for  $3\text{NaBH}_4\text{-GdF}_3$  composite to release 3.0 wt% of hydrogen is only 9 min in the 1<sup>st</sup> cycle. Interestingly, a drastic improvement on desorption kinetics upon cycling is achieved by showing the shifts of the dehydrogenation curves to the shorter time with increasing cycle numbers. For instance, to release 3.0 wt% of hydrogen, the time needed in the 2<sup>nd</sup> and 3<sup>rd</sup> cycles is reduced to 2 min, respectively. In addition, the total hydrogen contents released from the  $3\text{NaBH}_4\text{-GdF}_3$  composite are all about 3.50 wt% for the 1<sup>st</sup>, 2<sup>nd</sup> and 3<sup>rd</sup> cycles, which corresponds well with the absorbed ones in the first 3 rehydrogenation cycles, confirming a complete dehydrogenation for each cycle.

## References

- 1 L. N. Chong, J. X. Zou, X. Q. Zeng and W. J. Ding, *J. Mater. Chem. A*, 2014, **2**, 8557–8570.
- 2 L. N. Chong, J. X. Zou, X. Q. Zeng and W. J. Ding, *J. Mater. Chem. A*, 2013, **1**, 13510 - 13523.
- 3 L. N. Chong, J. X. Zou, X. Q. Zeng and W. J. Ding, *Int. J. Hydrogen Energy*, 2014, **39**, 14275-14281.
- 4 K. y. Li and D. f. Xue, *J. Phys. Chem. A*, 2006, **110**, 11332-11337.
- 5 A. Roine, *Outokumpu HSC Chemistry for Windows: Chemical Reaction and Equilibrium Software with Extensive Thermodynamical Database and Flowsheet Simulation, Version 5.1*, 02103-ORC-T, Outokumpu Research Oy, Finland, 2002.
- 6 Y. H. Guo, X. B. Yu, L. Gao, G. L. Xia, Z. P. Guo and H. K. Liu, *Energy Environ. Sci.*, 2010, **3**, 465-470.
- 7 G. Barkhordarian, T. Klassen, M. Dornheim and R. Bormann, *J. Alloys Compd.*, 2007, **440**, L18-L21.
- 8 R. Gosalawit-Utke, J. M. Bellosta von Colbe, M. Dornheim, T. R. Jensen, Y. Cerenius, C. B. Minella, M. Peschke and R. Bormann, *J. Phys. Chem. C*, 2010, **114**, 10291-10296.
- 9 J. Yang, A. Sudik and C. Wolverton, *J. Phys. Chem. C*, 2007, **111**, 19134-19140.
- 10 S. -A. Jin, Y. -S. Lee, J. -H. Shim and Y. W. Cho, *J. Phys. Chem. C*, 2008, **112**, 9520-9524.
- 11 L. N. Chong, J. X. Zou, X. Q. Zeng and W. J. Ding, *J. Mater. Chem. A*, 2013, **1**, 3983-3991.
- 12 K. y. Li and D. f. Xue, *J. Phys. Chem. A*, 2006, **110**, 11332-11337.